An observer-based approach for sensors (position/speed, currents and DC-link voltage) fault detection and diagnosis in PMSM drive

Sidath Diao, Demba Diallo, Claude Marchand

Group of Electrical Engineering Paris (GeePs) CNRS, CentraleSupélec, UPMC University Paris Sud, 11 rue Joliot Curie
91192 Gif Sur Yvette, France
demba.diallo@geeps.centralesupelec.fr

ABSTRACT. *The paper describes a strategy for the mechanical, current and DC bus voltage sensor Fault Detection and Diagnosis (FDD) of a Permanent Magnet Synchronous Machine (PMSM) drive. The method is based on three observers. The Extended Kalman Filter (EKF) is designed to estimate the position in case of mechanical sensor fault. A Model Reference Adaptive System (MRAS) estimates the phase currents using the actual position and speed and a nonlinear observer computes the DC link voltage from the phase currents and the duty cycles. The computation and sort of the residuals (difference between measured and estimated values) allows the fault isolation. The method is evaluated on a test bench with mechanical, phase current and DC voltage sensor faults. The experimental results show the effectiveness and the capability of fault detection and diagnosis of the proposed strategy.*

RÉSUMÉ. *Ce travail présente une méthodologie de détection et de diagnostic de défauts de capteur mécanique, de capteur de courant de phase ou de capteur du bus de tension continue pour un actionneur électrique à machine synchrone à aimants permanents. Elle s'appuie sur trois observateurs : un filtre de Kalman étendu pour l'estimation de la position du rotor, un modèle de référence adaptatif pour estimer les courants de phase et un observateur non linéaire pour estimer la tension du bus continu. La comparaison des estimations avec les valeurs mesurées permet de générer des résidus dont l'analyse permet le diagnostic et la localisation du défaut. La méthodologie est évaluée en insérant des défauts dans les valeurs mesurées sur un banc expérimental équipé d'une machine synchrone à aimants permanents de 15kW piloté par un système dSpace. Les résultats obtenus montrent l'efficacité de l'approche aussi bien sur la rapidité de la détection que la robustesse du diagnostic.*

KEYWORDS: *fault detection, fault isolation, PMSM drive, non linear observers, extended Kalman filter, Lyapunov functions.*

MOTS-CLÉS: *détection de défaut, localisation de défaut, observateur non linéaire, filtre de Kalman étendu, fonction de Lyapunov, machine synchrone à aimants permanents.*

DOI:10.3166/EJEE.17.455-473

1. Introduction

During the last decade, fault tolerant control has become an increasingly interesting topic in numerous industry domains (Benbouzid *et al.*, 2007). This is due to the increasing need of system availability, which target to keep under control the maximum of system operation hazards. Consequently, strategies are defined from the early preliminary design steps, so as to facilitate fault detection, fault isolation and control reconfiguration. In the automotive environment, electrical drives are more and more present and fulfill more and more functionalities. To make them available, both hardware design and control strategies should be considered. In fact, several recent works (Bennett *et al.*, 2011; Gaeta *et al.*, 2012) deal with robust and fault tolerant control of electrical drives. They are aimed at proposing new control strategies that ensure the continuity of operation despite the occurrence of faults.

A method widely used for Fault Detection and Isolation in AC drives is the observer-based method (Chen *et al.*, 1999; Campos-Delgado *et al.*, 2008). For position/speed sensor diagnosis, different methods have been successfully applied (Diao *et al.*, 2013a; Wallmark *et al.*, 2007; Green *et al.*, 2003). A complete Fault detection and fault-tolerant control of interior permanent-magnet motor drive system is presented in (Jeong *et al.*, 2005; Foo *et al.*, 2013; Najafabadi *et al.*, 2011) where a power equation is used to diagnose a DC Link voltage fault. However, this method could not be applicable in particular conditions such as steady state. In this paper, a new DC voltage observer is designed using phase currents and inverter control signal. For the phase currents, (Nuno *et al.*, 2014) proposes a simple detection approach based only on the currents measurements, however only open-loop control system is considered. Also, perform efficient sensor fault detection in harsh transient phase (speed or torque) is still a facing challenge.

Hereafter, the main components of a sensor-fault tolerant control strategy are detailed. It is applied to an electrical drive, composed of an inverter and a Permanent Magnet Synchronous Machine (PMSM). The drive could be used in transportation applications such as for example the electrical powertrain or the air conditioning (AC) of electric or hybrid electric vehicle (EV or HEV).

In the paper, position/speed sensor, the phase currents and the DC link voltage sensors are involved using three interconnected observers. In section II, after a brief recall on PMSM diagnosis needs, the cases of the position/speed sensor, currents sensors and the DC-link voltage sensor are respectively treated and illustrated with experimental results. Then, a conclusion gives the main advantages of this structure.

2. Sensor fault diagnosis for PMSM

As high reliability and robustness for various vehicle-operating conditions are prime considerations in EV or HEV propulsion, PMSM are becoming very attractive. Their operation is highly dependent on feedback sensors availability.

When a feedback signal is lost, a standard control fails or is significantly disturbed. In the same conditions, a Fault Tolerant Control (FTC) ensures continuous system operation even with diminished performances. A Fault Detection and Diagnosis (FDD) module detects the loss of the sensor and the FTC reconfigures the control to sustain the best control performances.

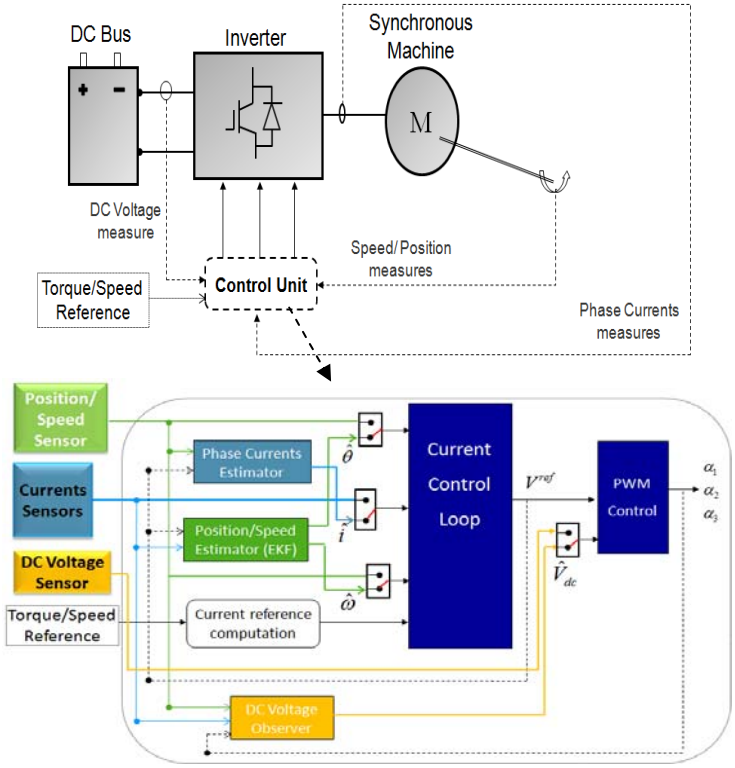

Figure 1. Fault tolerant control structure in a PMSM drive

With the aim of reaching the required level of availability in transportation applications, the drive is equipped with a DC voltage sensor, three current sensors (due to safety requirements in electric vehicle standards) and a position sensor. The speed is usually computed from the position. In order to enhance the reliability of the system regarding its sensors, hardware and software redundancy are usually adopted. Hardware redundancy adds complexity in the design and increases the system cost. Despite the computational over cost, software redundancy has become a promising alternative. This solution is much more attractive because of its flexibility and its capability of evolution. Thus, state, output or parameter estimation seems to be a suitable tool of the FDD. State estimation-based observers are suitable for fault detection since they cause a very short time delay in the real-time decision-

making process (Isermann, 2011) and offer a quick detection of sensor failures: under measurement, over measurement, high saturation, low saturation and complete outage. For this purpose, the signals are estimated through three software sensors based on the theory of observers: an Extended Kalman Filter (EKF), a Model Reference Adaptive System (MRAS) and a nonlinear observer for the DC link voltage estimation. A voting algorithm is used to enable the fault detection and to make the selection decision between measured and estimated values.

The objective is to have a system, which can adaptively reorganizes itself at sensor failure occurrence. The output of the faulty sensor is replaced by a signal derived from the control and the remaining sensors. The FTC structure in the PMSM drive already presented in (Diao *et al.*, 2013b), is displayed in Figure 1. The reconfiguration (nested in the Current Control Loop) is based on voting algorithms. They are designed to select the most relevant or appropriate value, which must be used by the current control loop.

2.1. Position sensor fault detection

Thereafter, the diagnosis of position/speed sensor mentioned above is developed with theoretical details and experimental results.

2.1.1. Position/speed observer synthesis

In PMSM drives, a position sensor is used, and generally, the speed is computed afterward by numeric means. The salient PMSM is modeled in the standard (*d,q*) reference frame as follows:

$$\frac{d}{dt}\begin{bmatrix} i_d \\ i_q \\ \omega \\ \theta \end{bmatrix} = \underbrace{\begin{bmatrix} -\frac{R_s}{L_d} & \frac{L_q}{L_d}\omega & 0 & 0 \\ -\frac{L_d}{L_q}\omega & -\frac{R_s}{L_q} & -\frac{\phi}{L_q} & 0 \\ 0 & 0 & 0 & 0 \\ 0 & 0 & 1 & 0 \end{bmatrix}}_{A} \begin{bmatrix} i_d \\ i_q \\ \omega \\ \theta \end{bmatrix} + \underbrace{\begin{bmatrix} \frac{\cos(\theta)}{L_d} & \frac{\sin(\theta)}{L_q} \\ -\frac{\sin(\theta)}{L_q} & \frac{\cos(\theta)}{L_d} \\ 0 & 0 \\ 0 & 0 \end{bmatrix}}_{B} \begin{bmatrix} v_\alpha & v_\beta \end{bmatrix} \quad (1a)$$

$$y = \underbrace{\begin{bmatrix} \cos(\theta) & -\sin(\theta) & 0 & 0 \\ \sin(\theta) & \cos(\theta) & 0 & 0 \end{bmatrix}}_{C} \begin{bmatrix} i_d \\ i_q \\ \omega \\ \theta \end{bmatrix} \quad (1b)$$

Where $x = [i_d, i_q, \omega, \theta]$, $u = [v_\alpha, v_\beta]$ $y = [i_\alpha, i_\beta]$

In these equations, v_α, v_β, i_α and i_β are respectively the voltages and currents in the (α,β) frame, i_d and i_q are the currents in the synchronous rotating (*d,q*) frame. L_d and L_q are respectively the direct and quadrature stator inductances, R_s is the stator

winding resistance, and ϕ is the flux produced by the magnets. ω is the angular velocity measured in electrical radians per second and θ is the electrical position. The objective is to provide an efficient back-up solution when the mechanical sensor fails.

There are three ways to provide an estimate of the mechanical information (position/speed). The first one is knowledge-based (such as artificial intelligence, genetic algorithms, fuzzy logic, etc.) which requires data recorded on the process to train the networks or design the rules (Maiti *et al.*, 2012; Orlowska-Kowalska *et al.*, 2010). The second one is the physical-model based approach that uses observers (Luenberger, Extended Kalman Filter, Sliding Mode Observer, Differential Algebraic, etc.) (Zaltni *et al.*, 2010; Sarikhani *et al.*, 2012; Diao *et al.*, 2015c). These techniques are mostly efficient for high speeds and may require a high computational cost. They can also suffer from the modeling errors or assumptions assumed for designing the analytical model. The third way is to inject High Frequency Signal. This technique requires an additional supply and the electrical machine must exhibit some particular properties such as magnetic saliency. Moreover the tuning may be tricky because of the additional losses and the increase of torque ripples (Zhu *et al.*, 2011; Bolognani *et al.*, 2011; Medjmadj *et al.*, 2015).

Hereafter, we use a model-based approach and a stochastic observer namely the Extended Kalman Filter (EKF) (Akrad *et al.*, 2011). This is a good compromise as the EKF has acceptable performances on the whole speed range. In fact at high speed an EMF-based observer would be more relevant but as its performances drastically reduce as the speed decreases it would have been mandatory to engage another at low speed another estimator. For sake of simplicity we have therefore decided to use a single estimator.

Estimation of the speed and the position is done using the reference voltages and phase currents sensors, which are uncorrelated from the mechanical sensor. Notice the fact that using uncorrelated sources is a key point of fault detection and reconfiguration.

For the digital implementation of an estimator, a discrete-time state-space model is required. Assume that the input vector u is nearly constant during a sampling period T_s, a first-order series expansion of the matrix exponential is used to discretize the model:

$$e^{AT_s} \approx A_d = I + AT_s \,,\; A^{-1}(e^{AT_s} - I)B \approx B_d T_s$$

The previous continuous model leads to the following discrete-time state-space model:

$$\begin{aligned} x(k+1) &= A_d x(k) + B_d u(k) \\ y(k) &= C_d x(k), C_d = C \end{aligned} \tag{2}$$

$$A_d = \begin{bmatrix} 1-\frac{R_s}{L_d}T_s & \frac{L_q\omega}{L_d}T_s & 0 & 0 \\ -\frac{L_d\omega}{L_q}T_s & 1-\frac{R_s}{L_q}T_s & -\frac{\phi}{L_q}T_s & 0 \\ 0 & 0 & 1 & 0 \\ 0 & 0 & T_s & 1 \end{bmatrix},\ B_d = \begin{bmatrix} \frac{\cos(\theta)}{L_d}T_s & \frac{\sin(\theta)}{L_q}T_s \\ -\frac{\sin(\theta)}{L_q}T_s & \frac{\cos(\theta)}{L_d}T_s \\ 0 & 0 \\ 0 & 0 \end{bmatrix}$$

A_d is the evaluation matrix and B_d the control matrix. The application of the EKF to the synchronous machine model is described as follows with the prediction and correction steps.

Prediction:

$$\begin{aligned} \hat{x}(k/k-1) &= A_d(k-1)\hat{x}(k-1/k-1) + B_d(k-1)u(k-1) \\ \Sigma(k/k-1) &= A(k-1)\Sigma(k-1/k-1)A(k-1)^T + Q(k-1) \end{aligned} \tag{3}$$

Correction

$$\begin{aligned} K(k) &= \Sigma(k-1)C_d{}^T(k)\left(C_d(k)\Sigma(k-1)C_d{}^T(k) + R(k)\right)^{-1} \\ \Sigma(k/k) &= \Sigma(k/k-1) - K(k)\,C(k)\Sigma(k/k-1) \\ \hat{x}(k/k) &= \hat{x}(k/k-1) + K(k)\left[y(k) - C_d(k)\hat{x}(k/k-1)\right] \end{aligned} \tag{4}$$

In (3) and (4), the covariance matrices Q and R characterize the noises that take into account the model approximations and the measurement errors. Without additional information, the noises are considered as uncorrelated, time independent and free-tuning parameters. Σ represents the variance matrix of the observation error and K is the observer gain matrix. The Kalman Filter-based estimator uses the equivalent two-phase currents measurements (i_α, i_β) and the control voltages (v_α, v_β) represented in the stationary reference frame to estimate the rotor position and speed, respectively $\hat{\theta}$ and $\hat{\omega}$. The estimation is done in a way that minimizes the mean of the quadratic error Σ between the measured phase currents and the estimated ones by taking into account the measurement noise and modelling errors.

2.1.2. Experimental Validation

The PMSM which characteristics are given in the appendix is fed through a Voltage Source Inverter and the algorithms are run on dSpace 1103. The switching frequency of the inverter is 20 kHz.

After numerous experimental trials, it was found that for mechanical position errors lower than +0.1 radian, the controllers were able to cope with the fault. Beyond this value undesirable effects arise and the fault detection becomes mandatory. Therefore this value will be used as a threshold to evaluate the EKF-

based fault detection effectiveness. The results are displayed within a reduced time range so as to have a better view of the position tracking.

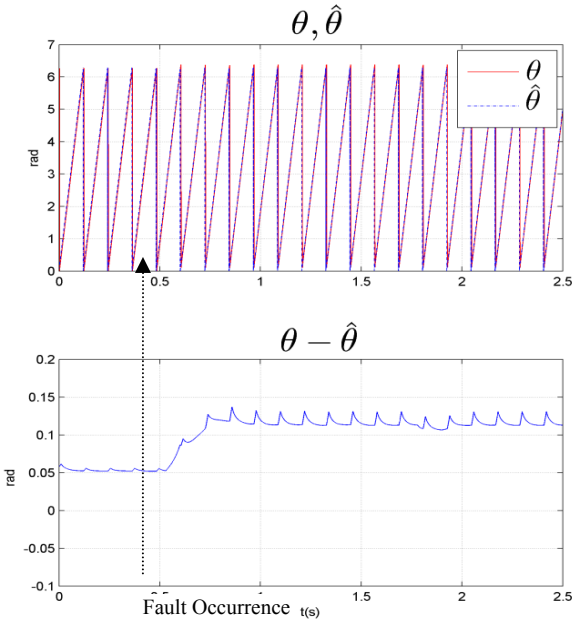

a) Measured, estimated and estimation error position

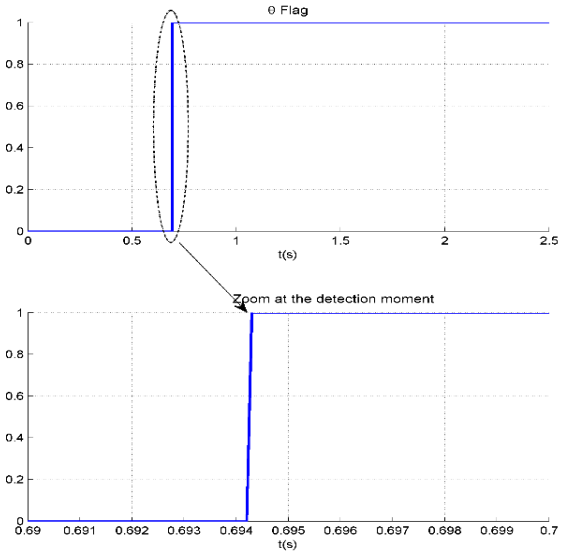

b) Position Sensor flag

Figure 2. Position sensor fault detection with EKF

At the fault occurrence (t = 0.53s), the estimation error (Figure 2a) varies significantly. The detection of the position sensor fault is then accomplished as indicated with the flag displayed in Figure 2b with a detection time duration Δt = 0.164 s.

The setting of the threshold value, which impacts the fault detection performance, is guided by the observer accuracy. The speed estimation error (Figure 3) is not really affected: only a peak of 2 rd/s (4% error) at the fault time appears before the error returns to its initial value.

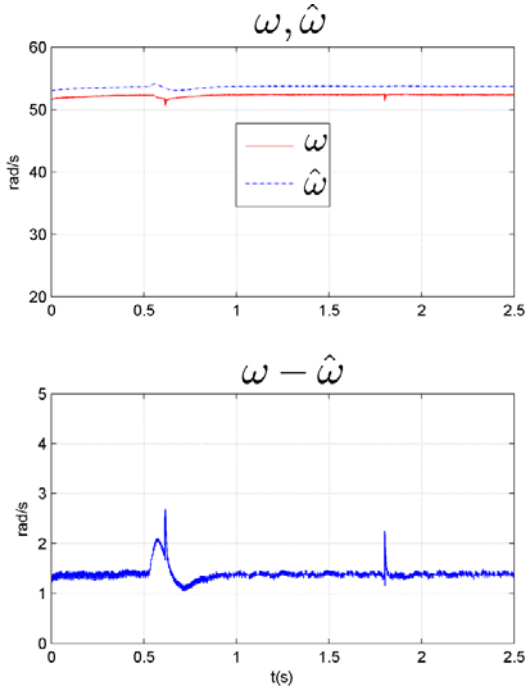

Figure 3. Measured and estimated speed, estimation error

Roughly speaking, an adaptive threshold can be settled for different operating point by analyzing the estimation error.

2.2. Current sensor fault diagnosis

At the apparition of a current sensor fault, a variation of the concerned phase current is expected and the goal is to spot quickly this variation so as to ensure an efficient fault tolerant control (Lee *et al.*, 2011; Rothenhagen *et al.*, 2009). The severity of the distortion from normal waveform depends mainly on the type of

fault. Because the currents estimated by the EKF for the position/speed estimation tends to converge to the values given by the current sensors by design of the EKF, they can't be used for current sensor fault diagnosis. So, current estimation must be completely uncorrelated from phase currents sensors.

2.2.1. Current observer synthesis

Considering the PMSM model, phase currents can be expressed as function of voltages, speed and position. Then, the residuals are obtained by making the difference between the estimated values and the measurements. Theoretically, the MRAS computes a desired state using two different models (*i.e.* reference and adjustable models). The reference model determines the desired states (phase currents) and the adjustable model generates the estimated values of the states. The PMSM model described in (1) with currents as states variables is now considered:

$$\frac{d}{dt}\begin{bmatrix} x_1 \\ x_2 \end{bmatrix} = \underbrace{\begin{bmatrix} -\frac{R_s}{L_d} & \frac{L_q\omega}{L_d} \\ -\frac{L_d\omega}{L_q} & -\frac{R_s}{L_q} \end{bmatrix}}_{A}\begin{bmatrix} x_1 \\ x_2 \end{bmatrix} + \underbrace{\begin{bmatrix} \frac{1}{L_d} & 0 \\ 0 & \frac{1}{L_q} \end{bmatrix}}_{B}\begin{bmatrix} u_d \\ u_q \end{bmatrix} \tag{5}$$

Where $x = [x_1, x_2] = [i_d + \frac{\phi}{L_d}, i_q]$ and $u = [u_d, u_q] = [u_d + \frac{R_s}{L_d}\phi, u_q]$

The control law by state feedback is: $u = -Kx$ where $K = [k_1, k_2]$ is the state feedback gain.

The system can now be written:

$$\frac{d}{dt}x = (A - BK)x \tag{6}$$

Stability analysis:

For a nonlinear system, the existence of Lyapunov functions is a sufficient condition for asymptotic stability. A Lyapunov function V is a positive definite function and has a Lie-derivative $\dot{V}$, which is negative definite.

For the nonlinear PMSM system, a candidate for a Lyapunov function is:

$$V(x) = \frac{1}{2}(x_1^2 + x_2^2) \text{ with } V(x) \geq 0 \tag{7}$$

$$\dot{V} = x_1\dot{x}_1 + x_2\dot{x}_2$$

$$\dot{V} = -\frac{1}{L_d}(R_s + k_1){x_1}^2 - \frac{1}{L_q}(R_s + k_2){x_2}^2 + x_1x_2(-\frac{k_1 + L_d\omega}{L_q} + \frac{L_q\omega - k_2}{L_d}) \tag{8}$$

K is chosen as follows: $k_1 = -L_d\omega$, $k_2 = L_q\omega$. The electrical parameters R_s, L_d and L_q are positive. Regarding the sign of the speed, the existence of the Lyapunov function is studied:

$$\dot{V} = -\frac{1}{L_d}(R_s - \omega L_d)x_1{}^2 - \frac{1}{L_q}(R_s + \omega L_q)x_2{}^2$$

- $\omega > 0$: if $L_d\omega < R_s$,then $\dot{V} < 0$ else if $\omega > \frac{R_s}{L_d}$ implies $\frac{1}{L_q}(R_s + \omega L_q)x_2{}^2 > \frac{1}{L_d}(R_s - \omega L_d)x_1{}^2$ then $\dot{V} < 0$
- $\omega < 0$: In the same way as previously, we have also $\dot{V} < 0$
- $\omega = 0$: $\dot{V} = -\frac{1}{L_d}(R_s)x_1{}^2 - \frac{1}{L_q}(R_s)x_2{}^2 < 0$

So for every operating speed, $\dot{V}$ is always negative and the closed loop is then asymptotically stable. So, the currents in the natural frame (*a,b,c*) can be estimated by applying the Park transformation with the estimated currents $[\hat{i}_a, \hat{i}_b, \hat{i}_c]$.

2.2.2. Experimental validation

Tests are done with a load torque of 0.5 Nm that is 15% of the nominal torque. An offset of 0.5 A (20% of the peak to peak current value) is inserted during operation in the phase B current from t = 2.05s to t = 6s. Figure 4 displays the speeds (the actual one computed from the measured position and the estimated speed by the EKF) and the phase B current. We can notice that despite the current sensor fault, the estimation of the speed is not affected.

In Figure 5, the three residuals $[i_a - \hat{i}_a, i_b - \hat{i}_b, i_c - \hat{i}_c]$ are plotted. The absolute value of the threshold (chosen according to the estimation error) for each phase is set at *0.18A* (dashed lines in Figure 5). The most important variation is observed in the second residual indicating that the fault affects Phase B sensor. The corresponding flags are plotted in Figure 6.

The fault detection time duration is Δt = 0.098s. For the reconfiguration when using only two sensors, a vector control can be used as reported in (Verma *et al.*, 2013) with a single sensor.

The variations in the two remaining phases are due to the closed loop operation. From t = 7 to 8s, a speed transient is noticed and the phase current estimation is robust with respect to this variation. So the current observer is globally accurate during steady state and transients.

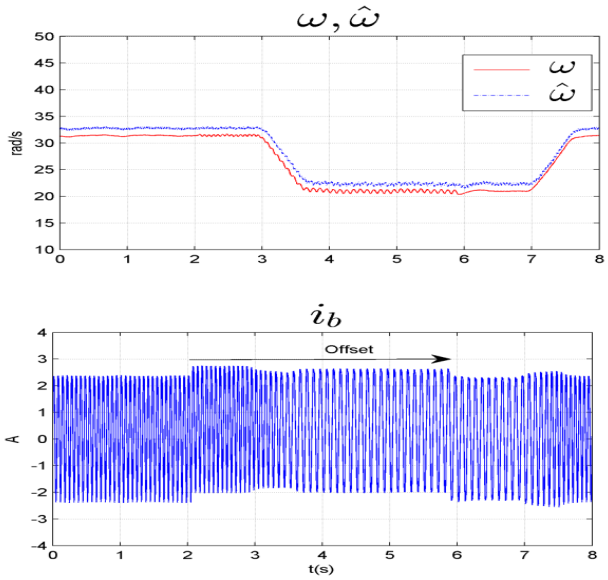

Figure 4. Mechanical speeds and Phase B current

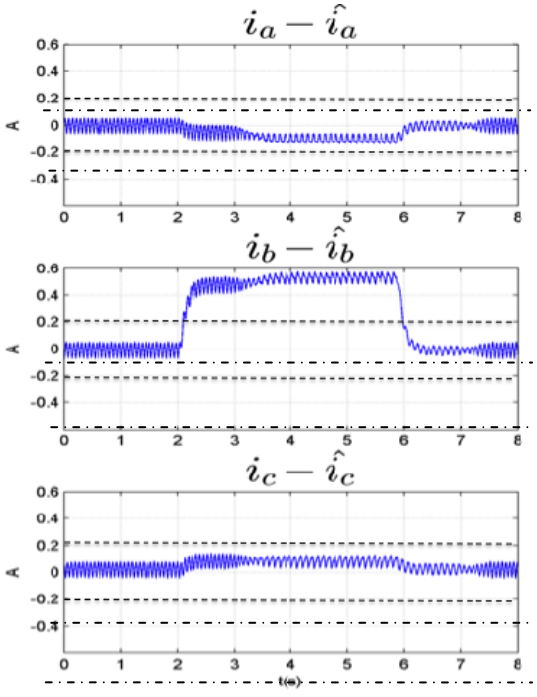

Figure 5. Current sensor fault Residuals

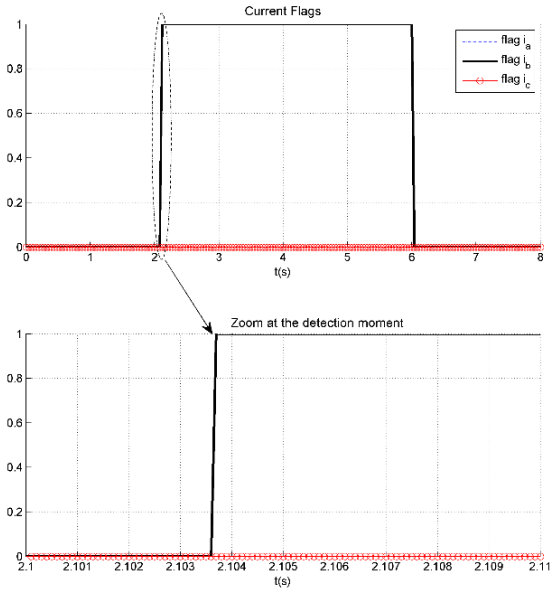

Figure 6. Current sensor flags

DC voltage sensor fault diagnosis

Actually, when the DC voltage sensor fails, the output of the Current Control Loop is modified and the PWM signal increases or decreases (positive offset/gain or negative offset/gain) to maintain the requested torque/speed. This leads to undesirable phase currents, which may affect the control performance or overheating the power converter or the machine windings. An observer can be a back-up solution when the DC voltage sensor fails to ensure the continuity of the operation with acceptable performance (Ohnishi *et al.*, 2004; Nademi *et al.*, 2011). One can also estimate the equivalent series resistance (ESR) of the DC-link electrolytic capacitor like in (Xing-Si *et al.*, 2013) to monitor the capacitor voltage. Voltage sensorless control method has also been applied in (Yip *et al.*, 2003) where a single current sensor is used to measure the inductor current and then give the inductor voltage. Then we are interested by the estimation of the DC-link voltage using the phase currents and the duty cycles. Firstly, the Kirchhoff law at the capacitor output is written. Then, using the voltage equation across the machine windings, a second-order system is defined according to Figure 7.

$$i = C\frac{dU_{dc}}{dt} = i_{DC/DC} - i_{DC/AC}, i_{DC/DC}, i_{DC/AC} = \sum_{j=1}^{3} i_j \alpha_j \qquad (9)$$

Under the assumption of the average model, the a-phase voltage can be written as:

$v_a = \alpha_1 U_{DC}$ where the α_j are the three half bridge control signals and i_j the phase currents.

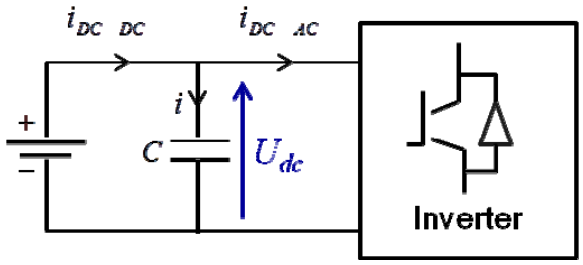

Figure 7. Inverter DC voltage bus layout

The dynamic of the DC link voltage and the A phase current can be written in a state space model as follows with e_a the phase electromotive force:

$$C\frac{dU_{dc}}{dt} = I_{DC/DC} - \alpha_1 i_a - \alpha_2 i_b - \alpha_3 i_c$$

$$L_a\frac{di_a}{dt} = -R_s i_a + v_a - e_a = -R_s i_a + \alpha_1 U_{dc} + \phi\omega\sin\theta$$

From this, the observer is synthesized:

$$\begin{aligned}\frac{d\hat{U}_{dc}}{dt} &= \frac{1}{C}(I_{DC/DC} - \alpha_1\hat{i}_a - \alpha_2 i_b - \alpha_3 i_c) + M_1(i_a - \hat{i}_a)\\ \frac{d\hat{i}_1}{dt} &= \frac{1}{L_a}(-R_s\hat{i}_a + \hat{U}_{dc}\alpha_1 - \phi\omega\sin\theta) + M_2(i_a - \hat{i}_a)\end{aligned} \tag{10}$$

Phase current estimation is used to correct the DC-link voltage estimation and compensate model uncertainties. The choice of M_1 and M_2 must be done according to the stability criterion. The tuning of M_1 and M_2 must be done according to the stability criterion. We first define the estimation errors: $\varepsilon_1 = i_a - \hat{i}_a, \varepsilon_2 = U_{DC} - \hat{U}_{DC}$. Then the dynamic of the estimation errors is given by:

$$\begin{aligned}\dot{\varepsilon}_1 &= -\frac{R_s}{L_a}\varepsilon_1 + \frac{\alpha_1}{L_a}\varepsilon_2 - M_2\varepsilon_1 = -(\frac{R_s}{L_a} + M_2)\varepsilon_1 + \frac{\alpha_1}{L_a}\varepsilon_2\\ \dot{\varepsilon}_2 &= \frac{\alpha_1}{C}\varepsilon_1 - M_1\varepsilon_1 = (\frac{\alpha_1}{C} - M_1)\varepsilon_1\end{aligned} \tag{11}$$

Assuming the following Lyapunov function: $V = \frac{1}{2}(\varepsilon_1^2 + \varepsilon_2^2) > 0$,

$$\dot{V} = \varepsilon_1\dot{\varepsilon}_1 + \varepsilon_2\dot{\varepsilon}_2 \Leftrightarrow \dot{V} = -(\frac{R_s}{L_a} + M_2)\varepsilon_1^2 + \varepsilon_1\varepsilon_2(\alpha_1(\frac{1}{L_a} + \frac{1}{C}) - M_1) \quad (12)$$

Choosing $M_1 = \alpha_1(\frac{1}{L_a} + \frac{1}{C})$ yields to $\dot{V} = -(\frac{R_s}{L_a} + K_2)\varepsilon_1^2 \le 0$ if $M_2 > 0$. So $\dot{V} \le 0$ and the closed loop system is then asymptotically stable with $M_1 = \alpha_1(\frac{1}{L_a} + \frac{1}{C}), M_2 > 0$.

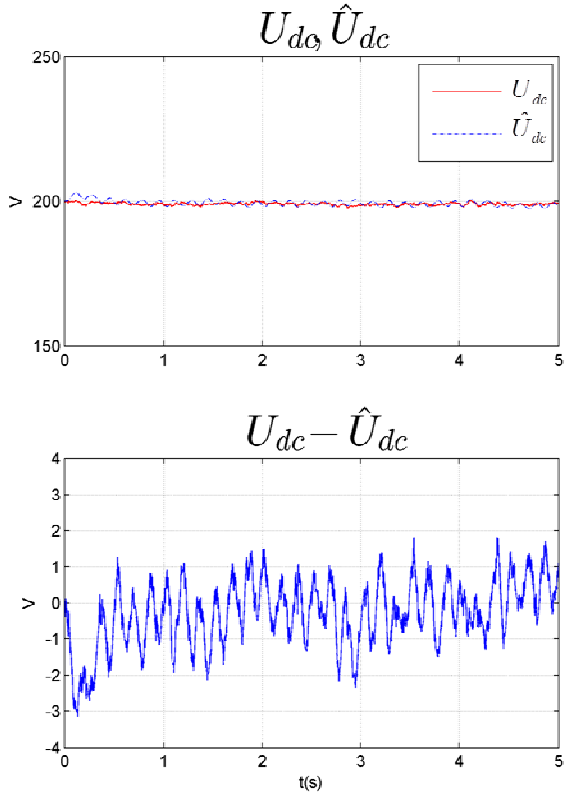

Figure 8. DC Voltage estimation at 200V

For the following experimental tests, we choose an experimental bench composed of a 3H bridge-level inverter connected to an AC grid with an electrical

machine of 15kW. The electrical machine is a non-salient PMSM with 4 poles pairs. The controller and the observer are sampled at 10kHz. Figure 8 shows the performances of the DC voltage tracking capabilities of the nonlinear observer with experimental tests. We notice a maximal estimation error of 1.5% for the observer.

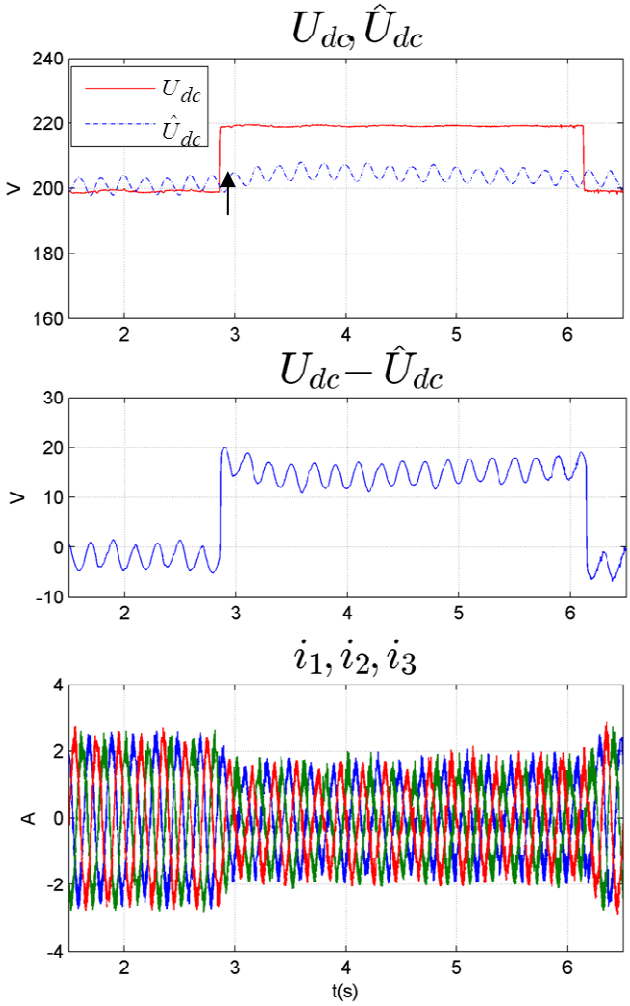

Figure 9. DC voltage estimation during a sensor fault

The test is done for the same operating point with a DC voltage of 200V during a sensor fault in Figure 9. An abrupt offset of 20 V representing 10% of the real value is introduced at time t =2.83s. The estimation error increases significantly as noticed in the second plot of the Figure 9 and sensor fault detection can be enabled. In the

same time, the measured currents are showed in the third plot of Figure 9 and the effect of the sensor fault is a decrease in the phase current magnitude.

The decrease in the currents magnitude is due to the fact that by over-measuring the DC voltage, the inverter requests less current than needed for the desired speed trajectory. Consequently, setting a threshold at *10 V* which means that an error of 5% on the nominal voltage is tolerated, a DC voltage sensor fault is detected in Figure 10 with a detection time duration $\Delta t = 0.058s$.

Then, as described in Figure 1, a complete sensor fault diagnosis structure is designed and validated for a PMSM drive. The inputs of this structure are the phase currents, the reference voltage and the PWM Control signals.

The last step of the fault tolerant control is the reconfiguration of the strategy. In case of a mechanical sensor fault, the estimated values with the EKF are used to ensure continuity of the operation. For current sensor fault the principle of balanced machine is used and the faulted phase current sensor is isolated and the measured value is computed from the two other healthy phase current sensors. For a DC link voltage sensor fault, the nonlinear observer could take over.

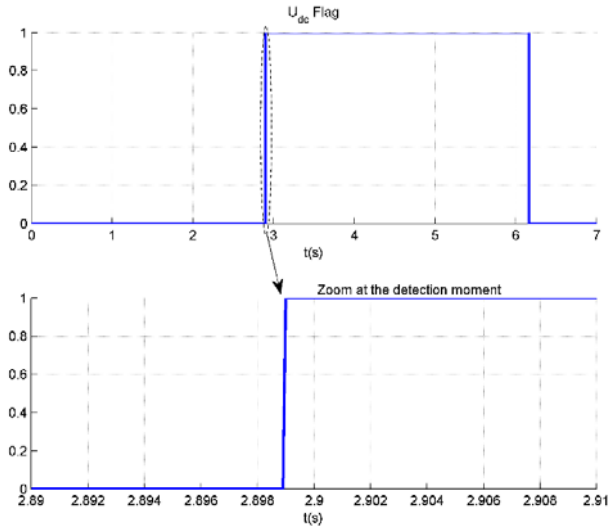

Figure 10. DC voltage sensor flag

3. Conclusion

This paper has described a sensor fault detection and diagnosis structure for a high-performance PMSM drive. The Fault Detection and Diagnosis is based on an Extended Kalman Filter (EKF), a Model Reference Adaptive System (MRAS), and a nonlinear observer. Thanks to the availability of analytical models, an observer-

based approach allows estimating the position/speed, the currents and the DC voltage despite the faults that may occur.

The structure allows selecting between the estimated values and the measured ones (position, speed, and phase currents) in case of sensor failure. The decision is made thanks to the computation of residuals. The main advantages are:

– Discrimination of a mechanical sensor fault from a phase current sensor fault thanks to the use of uncorrelated sources,

– Accurate current sensor fault detection and diagnosis with robustness to speed/torque variation.

Finally, the fault detection and diagnosis structure has shown his effectiveness through experimental results in case of a sensor (position, current or DC voltage) failure. The next step will be the implementation of the fault tolerant controller for online reconfiguration.

PMSM Parameters

Symbol	Definition	Value
P_n	Nominal power	1.1 kW
N_n	Nominal speed	3400 rev/min
T_n	Load torque	3.2 Nm
P	Pole pairs	3
In	Nominal current	5.9 A
R_s	Stator resistance	1.65 Ω
L_d	d axis inductance	3.5 10^{-3} H
L_q	q axis inductance	4.5 10^{-3} H
Ψ_m	Magnetic flux	154 10^{-3} Wb
f	Viscous friction	509 10 $^{-3}$ Nm/rad
J	Moment of inertia	6.4 10^{-3} kg/m²

Bibliography

Akrad A., Hilairet M., Diallo D. (2011). Design of a Fault-Tolerant Controller Based on Observers for a PMSM Drive. *Industrial Electronics, IEEE Transactions on*, vol. 58, n° 4, p. 1416-1427.

Benbouzid M.E.H., Diallo D., Zeraoulia M. (2007). Advanced Fault-Tolerant Control of Induction-Motor Drives for EV/HEV Traction Applications: From Conventional to Modern and Intelligent Control Techniques. *Vehicular Technology, IEEE Transactions on*, vol. 56, n° 2, p. 519-528.

Bennett J.W., Mecrow B.C., Atkinson D.J., Atkinson G.J. (2011). Safety-critical design of electromechanical actuation systems in commercial aircraft. *Electric Power Applications, IET*, vol. 5, n° 1, p. 37-47.

Bolognani S., Calligaro S., Petrella R., Tursini M. (2011). Sensorless Control of IPM Motors in the Low-Speed Range and at Standstill by HF Injection and DFT Processing. Industry Applications, *IEEE Transactions on*, vol.47, n° 1, p. 96-104.

Campos-Delgado D. U., Espinoza-Trejo D. R., Palacios E. (2008). Fault-tolerant control in variable speed drives: a survey. *Electric Power Applications, IET*, vol. 2, n° 2, p. 121-134.

Chen J., Patton R. (1999). *Robust model-based fault diagnosis for dynamic systems*. Kluwer Academic, Boston.

Diao S., Diallo D., Makni Z., Marchand C., Bisson J.F. (2013a). A differential algebraic approach for position/speed estimation in PMSM. Electric Machines & Drives Conference (IEMDC), *2013 IEEE International,* p. 1149-1154, 12-15 May, Chicago.

Diao S., Diallo D, Makni Z., Bisson J.F., Marchand C. (2013b). Sensor fault diagnosis for improving the availability of electrical drives. Industrial Electronics Society, IECON 2013, *39th Annual Conference of the IEEE*, p. 3108-3113.

Diao S., Diallo D., Makni Z., Marchand C., Bisson J.F. (2015). A Differential Algebraic Estimator for Sensorless Permanent Magnet Synchronous Machine Drive. *IEEE Transactions on Energy Conversion*, vol. 30, n° 1, p. 82-89.

Foo G.H.B., Zhang X., Vilathgamuwa D.M. (2013). A Sensor Fault Detection and Isolation Method in Interior Permanent-Magnet Synchronous Motor Drives Based on an Extended Kalman Filter. *IEEE Transactions on Industrial Electronics,* vol. 60, n° 8, p. 3485-3495

Gaeta A., Scelba G., Consoli A. (2012). Sensorless Vector Control of PM Synchronous Motors During Single-Phase Open-Circuit Faulted Conditions. *IEEE Transactions on Industry Applications,* vol. 48, n° 6, p. 1968-1979.

Green S., Atkinson D.J., Jack A.G., Mecrow B.C., King A. (2003). Sensorless operation of a fault tolerant PM drive. *Electric Power Applications, IEE Proceedings*, vol. 150, n° 2, p. 117-125.

Isermann R. (2011). *Fault Diagnosis Applications: Model Based Condition Monitoring, Actuators, Drives, Machinery, Plants, Sensors, and Fault tolerant Systems*. Springer, 1st Edition.

Jeong Y., Sul S., Schulz S., Patel N. (2005). Fault detection and fault-tolerant control of interior permanent-magnet motor drive system for electric vehicle. *IEEE Transactions on Industrial Applications*, vol. 41, n° 1, p. 46-51.

Lee B., Jeon N., Lee H. (2011). Current sensor fault detection and isolation of the driving motor for an in-wheel motor drive vehicle. *International conference on Control, Automation and Systems (ICCAS)*, 26-29 Oct., p. 486-491.

Maiti S., Verma V., Chakraborty C., Hori Y. (2012). An Adaptive Speed Sensorless Induction Motor Drive With Artificial Neural Network for Stability Enhancement. *Industrial Informatics, IEEE Transactions on*, vol.8, n° 4, p. 757-766.

Medjmadj S., Diallo D., Mostefai M., Delpha C., Arias A. (2015). PMSM Drive Position Estimation: Contribution to the High Frequency Injection Voltage Selection. *IEEE Transactions on Energy Conversion*, vol. 30, n° 1, March, p. 349-358.

Nademi H., Das A., Norum L. (2011). Nonlinear observer-based capacitor voltage estimation for sliding mode current controller in NPC multilevel converters. *PowerTech, IEEE Trondheim*, p.1-7, 19-23 June.

Najafabadi T., Salmasi F., Jabehdar-Maralani P. (2011). Detection and Isolation of Speed-, DC-Link Voltage and Current-Sensor Faults Based on an Adaptive Observer in Induction-Motor Drives. *IEEE Transactions on Industrial Electronics,* vol. 58, n° 5.

Nuno M. A. Freire, Estima J., Cardoso A. J. M. (2014). New Approach for Current Sensor Fault Diagnosis in PMSG Drives for Wind Energy Conversion Systems. *IEEE Transactions on Industry Applications*, p. 1206-1214.

Ohnishi T., Hojo M. (2004). DC voltage sensorless single-phase PFC converter. *IEEE Transactions on Power Electronics*, p. 404-410.

Orlowska-Kowalska T., Dybkowski M., Szabat K. (2010). Adaptive Sliding-Mode Neuro-Fuzzy Control of the Two-Mass Induction Motor Drive Without Mechanical Sensors. *Industrial Electronics, IEEE Transactions on*, vol. 57, n° 2, p. 553-564.

Rothenhagen K., F. Fuchs W. (2009). Current Sensor Fault Detection, Isolation, and Reconfiguration for Doubly Fed Induction Generators. *Industrial Electronics, IEEE Transactions on*, vol. 56, n° 10, p. 4239-4245.

Sarikhani A., Mohammed O.A. (2012). Sensorless Control of PM Synchronous Machines by Physics-Based EMF Observer. *Energy Conversion, IEEE Transactions on,* vol. 27, n° 4, p. 1009-1017.

Verma V., Chakraborty C., Maiti S., Hori Y. (2013). Speed Sensorless Vector Controlled Induction Motor Drive Using Single Current Sensor. *Energy Conversion, IEEE Transactions on*, vol. 28, n° 4, p. 938-950.

Wallmark O., Harnefors L., Carlson O. (2007). Control Algorithms for a Fault-Tolerant PMSM Drive. *Industrial Electronics, IEEE Transactions on*, vol. 54, n° 4, p. 1973-1980.

Xing-Si Pu, Nguyen T.H., Dong-Choon Lee, Kyo-Beum Lee, Jang-Mok Kim (2013). Fault Diagnosis of DC-Link Capacitors in Three-Phase AC/DC PWM Converters by Online Estimation of Equivalent Series Resistance. *Industrial Electronics, IEEE Transactions on*, vol. 60, n° 9, p. 4118-4127.

Yip S.C., Qiu D.Y., Chung H.S.H., Hui S.Y.R. (2003). A Novel Voltage Sensorless Control Technique for a Bidirectional AC/DC converter. *IEEE Transactions on Power Electronics*, p. 1346-1355.

Zaltni D., Ghanes M., Barbot J-P., Naceur A. (2010). Synchronous Motor Observability Study and an Improved Zero-speed Position Estimation Design. *IEEE Conference on Decision and Control, Atlanta.*

Zhu Z.Q., Gong L.M. (2011). Investigation of Effectiveness of Sensorless Operation in Carrier-Signal-Injection-Based Sensorless-Control Methods. *Industrial Electronics, IEEE Transactions on,* vol. 58, n° 8, p. 3431-3439.

Received: 8 March 2015
Accepted: 1 September 2015